Cancellation of laser phase fluctuations in Stokes and anti-Stokes generation

Z. W. Li, C. Radzewicz,* and M. G. Raymer†

The Institute of Optics, University of Rochester, Rochester, New York 14627

Received May 9, 1988; accepted July 1, 1988

In the coherent anti-Stokes Raman scattering process, the spectrum of the generated optical phonon depends on the degree of temporal correlation between the pump laser field and the Stokes field. When the two fields are strongly correlated, such as when the Stokes field is generated with stimulated Raman scattering (SRS), the spectral shape of the optical phonon is found experimentally and theoretically to be the same as the gain-narrowed Raman line shape because the laser phase fluctuations cancel out totally, leaving only the collisional noise in the SRS process. When the two fields are uncorrelated, the shape of the optical-phonon spectrum is found to be the same as the Raman line shape without gain narrowing. When two fields are partially correlated, then the two spectral components appear together. We provide a method to measure the degree of correlation between two optical fields that have different central frequencies. The theory developed to interpret the experimental results is an extension of the quantum theory of SRS to include anti-Stokes scattering. We show that only in the high-gain limit can the quantum fluctuations be thought of as arising from a classical noise process.

INTRODUCTION

It has been known for some time that if the pump and Stokes waves in a Raman amplifier have temporal phase fluctuations that are perfectly correlated, then the effect of those fluctuations cancels out, and the molecules respond as if being driven by monochromatic fields. The effect is easily understood because the Raman process depends on the *difference* of the pump and Stokes frequencies, which is constant in the presence of perfectly correlated phase (i.e., frequency) fluctuations. Thus we can say that a narrow-band optical phonon is produced by the correlated action of two broadband driving fields. This yields a Raman gain that is equal to that for the case of monochromatic fields. Theoretically, this phase cancellation was first pointed out by Carman *et al.*[1] and later was discussed in some detail by others.[2] These predictions for the Raman amplifier have not been tested for purely phase-fluctuating fields, but gain enhancement of similar origin has been predicted and observed for correlated *multimode* fields, in which amplitude fluctuations are dominant.[3,4] It has also been shown that a Raman amplifier can induce strong phase correlations between the fluctuating pump wave and the amplified Stokes wave in the absence of any such correlations at the input.[5]

In the case of the Raman generator, where the Stokes light builds up from spontaneous scattering, it is known that when the pump is broadband the Stokes light is generated with the same bandwidth as the pump field and automatically has strong correlation to the pump fluctuations.[4–8] This is because the spontaneous noise field contains all phases, and the amplification process picks out the correlated part, which has the highest gain. Thus Stokes generation is a convenient way to produce a frequency-shifted field that is well correlated with the pump field.[4,5,7,8] However, note that the degree of correlation approaches unity only when the rate of pump fluctuation is much larger than the Raman linewidth.[6–9]

The present paper presents a study of the effects of cross correlation between the broadband pump and Stokes waves in the coherent anti-Stokes Raman scattering (CARS) process. In a recent paper we reported the enhancement of the CARS gain by the effect of such a correlation.[10] This is distinct from other related studies, which considered correlation between the pump wave with center frequency ω_{L1} and the probe wave at ω_{L2}, whose sum is equal to the sum of Stokes and anti-Stokes frequencies, $\omega_{L1} + \omega_{L2} = \omega_S + \omega_{AS}$.[11] In our previous study the CARS gain enhancement arose from the same cancellation of pump and Stokes phase fluctuation as discussed above for the Raman amplifier. From this gain enhancement we could infer only that a narrow-band optical phonon was produced when the phases of the two fields were well correlated.

In the present study we present direct evidence for the generation of the narrow-band optical phonon by the action of broadband, phase-correlated fields. We also show that the narrow-band component of the phonon gradually disappears as the degree of cross correlation between pump and Stokes fields is decreased. This is accomplished by scattering a nearly monochromatic probe field $E_{L2}(t)$ at ω_{L2} off the phonon wave to produce coherent anti-Stokes scattering at ω_{AS}. The spectrum of the generated anti-Stokes wave is proportional to that of the phonon. This fact can be seen by examining the well-known coupled differential equations for the complex amplitudes of the anti-Stokes field $E_{AS}(t, z)$ and the optical phonon $Q(t)$:

$$\frac{\partial}{\partial z} E_{AS}(z, t) = -i\kappa_{2A} E_{L2}(t) Q(t) \exp(-i\Delta\mathbf{k} \cdot \mathbf{z}), \tag{1}$$

$$\frac{\partial}{\partial t} Q(t) = (i\Delta - \Gamma) Q(t) - i\kappa_1{}^* E_{L1}(t) E_S{}^*(t), \tag{2}$$

where $t = t_{lab} - z/c$ is the local time variable on which the external driving fields $E_{L1}(t)$, $E_S(t)$, and $E_{L2}(t)$ depend exclusively. Γ is the collisional dephasing rate for the Raman

0740-3224/88/112340-08$02.00

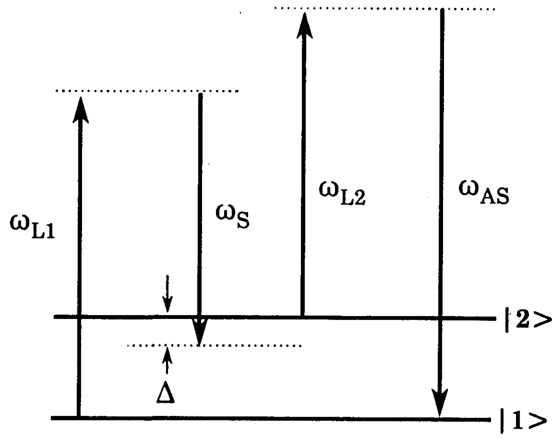

Fig. 1. Illustration of the CARS process. The frequencies (in radians per second) of pump laser ω_{L1}, generated Stokes field ω_S, monochromatic probe field ω_{L2}, and anti-Stokes field ω_{AS} satisfy $\omega_{L1} + \omega_{L2} = \omega_S + \omega_{AS}$. The detuning from Raman resonance is $\Delta = \omega_{21} - \omega_{L1} + \omega_S$, where ω_{21} is the Raman shift of the medium.

transition $|1\rangle \rightarrow |2\rangle$, $\Delta = \omega_{21} - \omega_{L1} + \omega_S$ as shown in Fig. 1, κ_1 and κ_{2A} are coupling constants,[12] and $\Delta\mathbf{k} = \mathbf{k}_{L1} + \mathbf{k}_{L2} - \mathbf{k}_S - \mathbf{k}_{AS}$ is the spatial phase mismatch, assumed to be zero. In the low-gain limit of the anti-Stokes generation process, Eq. (1) gives simply

$$E_{AS}(z, t) = -i\kappa_{2A}E_{L2}(t)Q(t)z. \quad (3)$$

If the probe wave $E_{L2}(t)$ is monochromatic, then the anti-Stokes field is seen to follow the phonon amplitude $Q(t)$; thus, measuring the spectrum of the anti-Stokes field gives information directly about the spectrum of the phonon wave.

EXPERIMENTAL STUDY

In order to study experimentally the effects of random phase fluctuation in the absence of amplitude fluctuation, we have used broadband, amplitude-stabilized chaotic light as the pump field $E_{L1}(t)$. This is the light from a cavityless, pulsed dye laser that has been amplitude stabilized by passage through two saturated amplifiers.[13] Whereas the rapid amplitude fluctuations during a single pulse are reduced to less than 5%, the rapid phase fluctuations remain the same as those of the input chaotic (thermal) light. The resulting field is similar to the so-called phase-diffusion light, which has a uniform phase distribution and a smooth average spectrum.[2] When the amplitude-stabilized chaotic field $E_{L1}(t)$ is used to pump a Raman generator, the Stokes field $E_S(t)$ produced by single-pass stimulated Raman scattering (SRS) also has nearly constant amplitude and rapid phase fluctuations, which are strongly correlated to those of the pump field.

A schematic representation of the experimental setup is shown in Fig. 2. Pulses of amplitude-stabilized chaotic light generated by the dye-laser system were 4 nsec in duration and had a bandwidth of approximately 9 GHz (FWHM), a pulse energy of 3 mJ, and a wavelength of 564 nm. The dye-

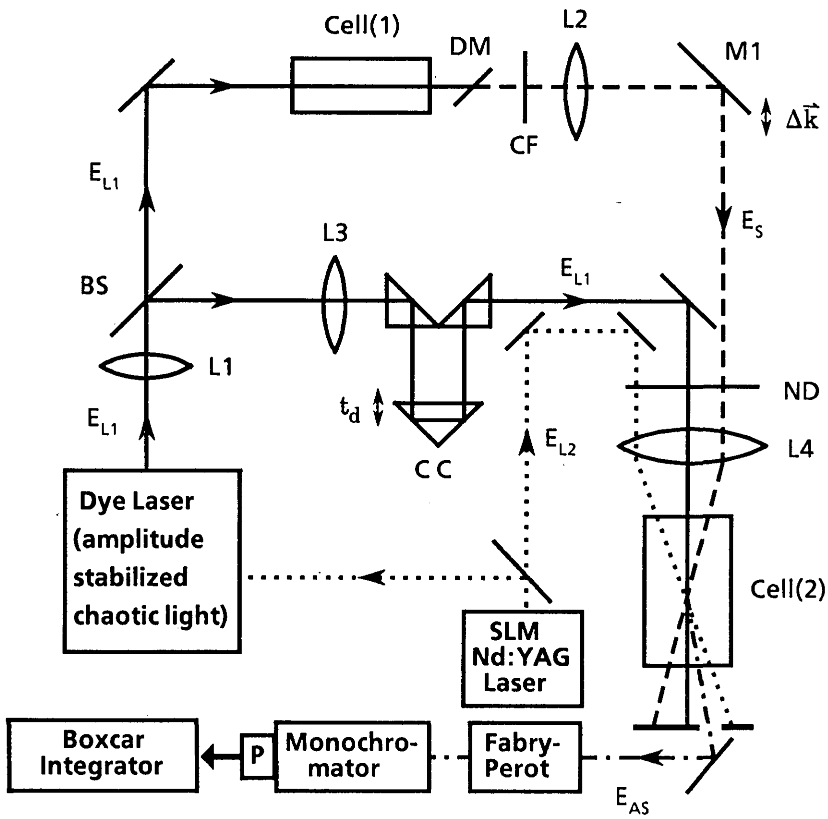

Fig. 2. Experimental setup. Stokes light generated in Raman generator Cell(1) is phase correlated to pump-laser field E_{L1}. The pump field is delayed by time t_d and combined with probe field E_{L2} in Cell(2). The anti-Stokes spectrum is measured with a Fabry–Perot interferometer and photodiode P: BS, beam splitter; DM, dichroic mirror, CF, colored-glass filter; ND, neutral-density filter; CC, corner cube; M1, mirror; L1–L4, lenses.

laser beam was divided into two parts by the beam splitter. The stronger beam (~80% of the total energy) was weakly focused with lens L1 down to 0.45 mm inside the Raman generator [Cell(1)], filled with H_2 at room temperature, producing phase-correlated Stokes light at 737 nm by vibrational SRS. The average energy of the Stokes pulses is 0.5 mJ for the pressure of 100 atm in Cell(1) and 0.3 mJ for the pressure of 48 atm. A dichroic mirror and a colored-glass filter were used to block the laser beam that copropagated with the generated Stokes beam. The 20% of the dye-laser beam that was deflected by the beam splitter was sent through a corner-cube delay line and used as the pump field for the CARS process in H_2 Cell(2). A probe-laser beam was derived from the frequency-doubled, single-longitudinal-mode Nd:YAG laser that was used to pump the dye laser. The probe beam had a pulse energy of 0.2 mJ, a bandwidth of approximately 50 MHz, a duration of 5 nsec, and a wavelength of 532 nm. The three beams $E_{L1}(t)$, $E_{L2}(t)$, and $E_S(t)$ were collimated and then focused by lens L4 into the four-wave mixing Raman H_2 Cell(2). The Raman resonance detuning Δ between the two Raman cells was determined by the difference in pressures in the two cells.[14] The coplanar phase-matching condition ($\mathbf{k}_{L1} + \mathbf{k}_{L2} = \mathbf{k}_S + \mathbf{k}_{AS}$) for generating anti-Stokes light H_2 Cell(2) was achieved by translating mirror M1 in the direction shown in Fig. 2. To prevent saturation in the CARS process, a neutral-density attenuator was inserted in front of lens L4. The anti-Stokes signal from Cell(2) was spectrally analyzed with a scanning Fabry–Perot interferometer controlled by a ramp generator. The signal from the Fabry–Perot interferometer was passed through a large-bandwidth monochromator to block stray light and then was detected by a photodiode (whose output was integrated by a boxcar integrator) and recorded and averaged with a microcomputer.

Curve 1 of Fig. 3 shows the ensemble-averaged spectrum of the amplitude-stabilized, chaotic dye-laser light, with a linewidth (FWHM) equal to 9.0 GHz. The spectra of individual pulses show strong random structure.[13] The averaged spectrum of the generated Stokes light also had a width of ~9 GHz. Curve 2 of Fig. 3 shows the average spectrum of the generated anti-Stokes light for the case of zero Raman detuning (both cells at 48 atm) and zero time delay between fields E_{L1} and E_S. The observed anti-Stokes linewidth is 0.70 GHz. As explained above, this shows directly that an optical phonon is produced with a linewidth much narrower than the spectra of the driving fields E_{L1} and E_S.

To obtain more insight into the effects of phase cross correlation, we varied the degree of cross correlation between pump and Stokes fields by varying the time delay t_d between E_{L1} and E_S by translating the corner cube. To make the effects clearer we also detuned the Raman resonance in Cell(2) from that in Cell(1) by an amount $\Delta = 3.8$ GHz by setting the pressure to 48 atm in Cell(2) and 100 atm in Cell(1).[14] Figures 4(a), 4(b), and 4(c) show the measured anti-Stokes spectra corresponding to optical delay between the pump laser and generated Stokes beam to be 3.3, 37, and 160 psec, respectively. It can be seen that there are two distinct components separated by approximately 3.8 GHz, which is equal to the Raman detuning. The narrower component has a linewidth of 1.4 GHz, and the broader component has a linewidth of 2.5 GHz, which is equal to the Raman linewidth in Cell(2).[14] The narrower one is dominant when the pump and Stokes fields are well correlated, and the broader one becomes significant when the two fields are partially decorrelated. Notice that the width of the narrower component does not change when the two fields become partially decorrelated. When the optical delay is large enough, the spectrum of the anti-Stokes light is essentially the same as the collision-broadened Raman transition.

The observed behavior can be understood qualitatively as follows: According to Eq. (2), the optical phonon $Q(t)$ is driven by an effective field, $E_e(t) \equiv E_{L1}(t)E_S^*(t)$, which is proportional to the so-called two-photon Rabi frequency for the effective two-level molecular transition $|1\rangle \rightarrow |2\rangle$.[2,15] The pump field can be written as

$$E_{L1}(t) = A_{L1} \exp[-i\phi_{L1}(t)], \tag{4}$$

where A_{L1} is a nearly constant amplitude and $\phi_{L1}(t)$ is the rapidly fluctuating phase. The Stokes field, generated by high-gain SRS in Cell(1) and time delayed by t_d, can be written as

$$E_S(t) = \xi(t - t_d)E_{L1}(t - t_d), \tag{5}$$

where $\xi(t)$ is a slowly varying random function accounting for the fact that collisional dephasing in the generator cell prevents the Stokes field from being perfectly correlated to the pump field.[6–8] Thus the effective field is

$$E_e(t) = |A_{L1}|^2\xi(t - t_d)\exp[-i\phi_{L1}(t) + i\phi_{L1}(t - t_d)]. \tag{6}$$

From this we can easily see that for zero delay time the pump phase fluctuations cancel out, leaving only the slower collisional fluctuations. Thus the effective driving field is narrow-band; this leads to the narrow spectral component at the detuned frequency in Fig. 4(a) and corresponds to the pro-

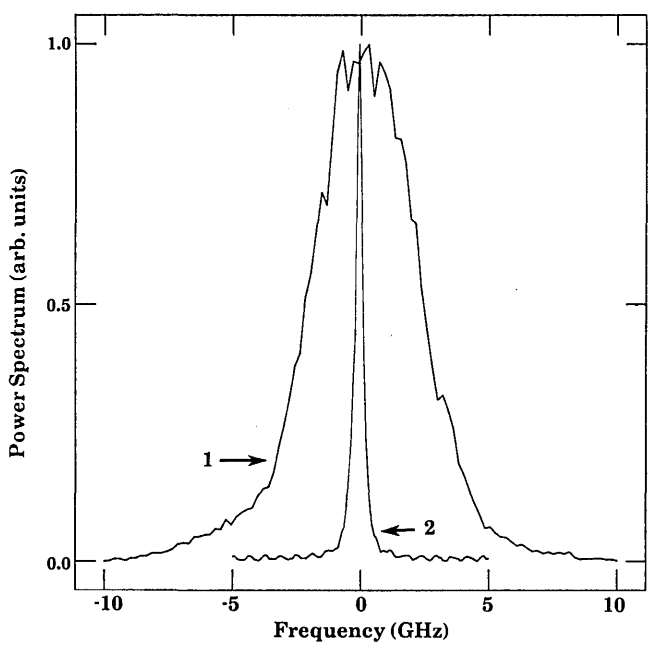

Fig. 3. Measured average power spectra of (curve 1) pump laser and (curve 2) the generated anti-Stokes field, for the case of zero Raman detuning (both cells at 48 atm). The narrow width of the anti-Stokes field illustrates the cancellation of the laser and Stokes phase fluctuations. The curves are normalized to a peak height of unity, and the horizontal scale is with respect to the center frequency of each field.

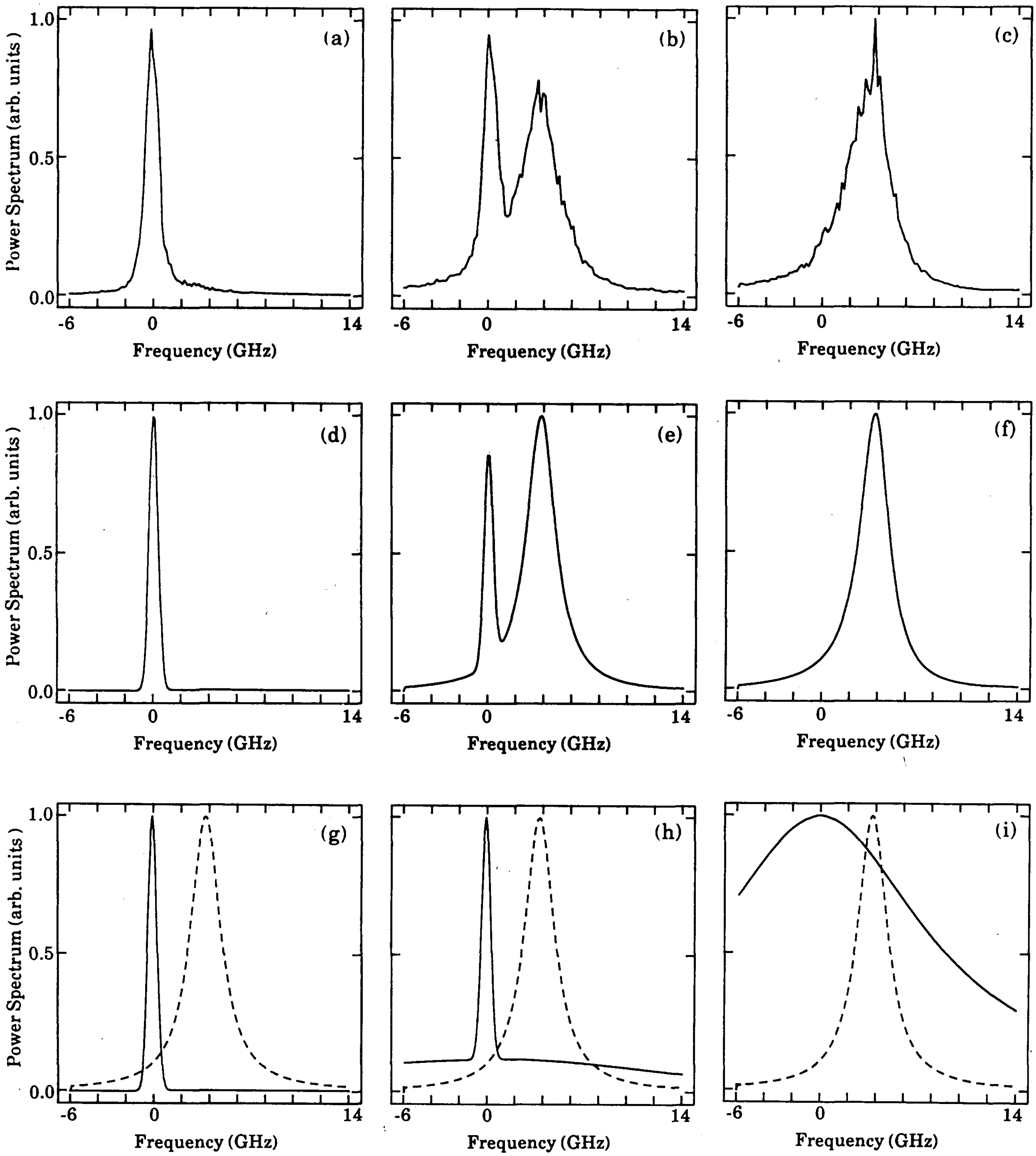

Fig. 4. Power spectra of anti-Stokes field for detuning of $\Delta = 3.8$ GHz and for various values of time delay t_d between pump and Stokes fields. The frequency scale is labeled with respect to the location of the narrow peak, which is predicted to occur at $\omega_{L1} + \omega_{L2} - \omega_S$. (a), (b), (c) Measured anti-Stokes spectra corresponding to delay t_d equal to 3.3, 37, and 160 psec, respectively. (d), (e), (f) Theoretical predictions for anti-Stokes spectra, evaluated by combining Eqs. (8) and (15), corresponding to the optical delay t_d in (a), (b), and (c), respectively. (g), (h), (i): Solid curves are the power spectra $S_e(\omega)$ of the effective driving field, evaluated using Eq. (15), corresponding to optical delay t_d in (a), (b), and (c), respectively. The dashed curves of (g), (h), and (i) are the Lorentzian Raman line shapes, which, when multiplied by the solid curve $S_e(\omega)$, give the corresponding spectra in (d), (e), and (f). Γ, Γ_1, Γ_{L1}, Δ, and gl are taken to be the same as the experimental parameters. All curves are normalized to a peak height of unity.

cess going through the virtual levels, shown as dotted lines in Fig. 1. On the other hand, when the delay time is much larger than the coherence time of $E_{L1}(t)$, the effective field has a spectral width roughly twice that of $E_{L1}(t)$. This leads to the broad spectral component at the resonant frequency in Fig. 4(c) because the four-wave mixing response is strongest there.

THEORY

A quantitative theory of this behavior can be developed as follows: Eq. (3) shows that the anti-Stokes field and optical phonon have the same spectrum if the probe beam is monochromatic. This spectrum can be found by integrating Eq. (2), which gives

$$Q(t) = -i\kappa_1{}^* \int_0^t \exp[(i\Delta - \Gamma)(t - t')]E_e(t')\mathrm{d}t'. \quad (7)$$

Then a straightforward calculation[16] shows that in the steady state the power spectrum $S_Q(\omega)$ of $Q(t)$ is given by

$$S_Q(\omega) = |\kappa_1|^2 \frac{1}{\Gamma^2 + (\omega - \Delta)^2} S_e(\omega), \quad (8)$$

where $S_e(\omega)$ is the power spectrum of the effective field $E_e(t)$. The power spectra are defined as

$$S_F(\omega) = \int_{-\infty}^{+\infty} \langle F(t + \tau)F^*(t)\rangle e^{-i\omega\tau}\mathrm{d}\tau, \quad (9)$$

where $F(t)$ is a stationary random process, such as $E_{L1}(t)$, $E_S(t)$, $Q(t)$, and $E_{AS}(t)$, and $\langle\ldots\rangle$ means an ensemble average. According to the definition of $E_e(t)$, its power spectrum is equal to

$$S_e(\omega) = \int_{-\infty}^{+\infty} \langle E_{L1}(t + \tau)E_S{}^*(t + \tau)E_{L1}{}^*(t)E_S(t)\rangle e^{-i\omega\tau}\mathrm{d}t, \quad (10)$$

where the generated Stokes field $E_S(t)$ can be written as Eq. (5). The $\xi(t)$ in Eq. (5) is, strictly speaking, a quantum fluctuation operator because the origin of the generated Stokes is spontaneous quantum noise.[6,7,9] However, in the high-gain limit of the SRS process we can treat $\xi(t)$ as a classical random process, at least for the purpose of calculating two-time correlation functions. This is proved in Appendix A. The corresponding power spectrum of $\xi(t)$ is shown there to be

$$S_\xi(\omega) = \frac{I_S}{I_{L1}} \frac{2(\pi gl)^{1/2}}{\Gamma_1} \exp\left(-\frac{gl}{\Gamma_1{}^2}\omega^2\right), \quad (11)$$

where $I_{L1} = |E_{L1}|^2$ is the pump laser intensity, $I_S = \langle|E_S|^2\rangle$ is the Stokes field intensity [Eq.(A12)], and g, l and Γ_1 are the gain coefficient, gain medium length, and collisional dephasing rate, respectively, in the SRS generator Cell(1). $S_\xi(\omega)$ is the spectrum of SRS in the case when the pump laser is monochromatic[6] and shows the effect of gain narrowing: the width decreases with increasing gl. As shown in Appendix A, the random variable $\xi(t)$ is statistically independent of $E_{L1}(t)$ if the pump field has only phase fluctuations. Therefore the power spectrum $S_e(\omega)$ of the effective field can be expressed as a convolution:

$$S_e(\omega) = \int_{-\infty}^{+\infty} \langle E_{L1}(t + \tau)E_{L1}{}^*(t - t_d + \tau)E_{L1}{}^*(t)E_{L1}(t - t_d)\rangle \times e^{-i\omega\tau}\mathrm{d}\tau \otimes S_\xi(\omega). \quad (12)$$

The calculation of the fourth-order autocorrelation function of the pump field in Eq. (12) can be carried out by using the phase-diffusion model[2] for $E_{L1}(t)$. This approximates our experimental situation because the amplitude-stabilized chaotic light has slowly varying amplitude and rapidly fluctuating phase with uniform distribution. In this model the laser-field autocorrelation is given by

$$\langle E_{L1}(t + \tau)E_{L1}{}^*(t)\rangle = |E_{L1}|^2 \exp(-\Gamma_{L1}|\tau|), \quad (13)$$

where $2\Gamma_{L1}$ is the bandwidth (FWHM) of the laser (in radians per second). The four-time correlation function is given by

$$\langle E_{L1}(t + \tau)E_{L1}{}^*(t - t_d + \tau)E_{L1}{}^*(t)E_{L1}(t - t_d)\rangle = I_{L1}{}^2 \exp[\Gamma_{L1}(|t_d + \tau| + |t_d - \tau| - 2|t_d| - 2|\tau|)]. \quad (14)$$

Then, the integral in Eq. (12) can be carried out to give

$$S_e(\omega) = I_{L1}I_S \frac{2(\pi gl)^{1/2}}{\Gamma_1} \left\{\exp(-2\Gamma_{L1}|t_d|)\left[2\pi\delta(\omega) - L(\omega) \times \cos(\omega|t_d|) - 2\Gamma_{L1}L(\omega)\frac{\sin(\omega|t_d|)}{\omega}\right] + L(\omega)\right\} \otimes \exp\left(-\frac{gl}{\Gamma_1{}^2}\omega^2\right), \quad (15)$$

where $L(\omega)$ is the self-convolution of the pump-field power spectrum and is equal to $4\Gamma_{L1}/[(2\Gamma_{L1})^2 + \omega^2]$ in the phase-diffusion model.

The optical-phonon power spectrum $S_Q(\omega)$ is then obtained by substituting Eq. (15) into Eq. (8) and can be simplified in two limiting cases. In the case of zero optical delay between pump and Stokes waves, the power spectrum of the optical phonon arises only from the delta-function term and becomes

$$S_Q(\omega, t_d \to 0) = |\kappa_1|^2 I_{L1}I_S \frac{4\pi(\pi gl)^{1/2}}{\Gamma_1} \frac{1}{\Gamma^2 + \Delta^2} \exp\left(-\frac{gl}{\Gamma_1{}^2}\omega^2\right), \quad (16)$$

where we have assumed that $\Gamma \gg \Gamma_1/(gl)^{1/2}$, and thus the Lorentzian is nearly constant over the small range of ω where $S_e(\omega)$ is peaked. According to Eq. (16), when $E_S(t)$ and $E_{L1}(t)$ are strongly correlated, the optical-phonon spectrum is the same as the gain-narrowed stimulated Raman line shape, Eq. (11), and is independent of the laser line shape. The spectral width (FWHM) is given by Eq. (16) to be $2\Gamma_1 (\ln 2/gl)^{1/2}$. For curve 2 of Fig. 3 this predicts a width of 0.35 GHz, and the observed width is 0.70 GHz. For the curve in Fig. 4(a) this predicts a width of 0.74 GHz, and the observed width is 1.4 GHz. The excess parts of the observed widths most likely are due to the finite resolution of the spectrometer used. For these calculations the collisional-broadening constant Γ_1 in the generator cell was taken to be equal to 7.9×10^9 rad/sec (1.25 GHz) for Fig. 3 and 1.6×10^6 rad/sec (2.6 GHz) for Fig. 4.[14] The length of the generator cell was l = 100 cm. The gain coefficient g, which was taken to be equal to 0.34/cm, was estimated in two ways. The first method was to measure the Stokes pulse energy (0.5 mJ) and duration (3 nsec) and then to use Eq. (A12) to obtain g. The second method was to measure the pump-laser pulse energy (2.4 mJ), duration (4 nsec), and average beam diameter (0.50 mm FWHM) in Cell(1) and then to use $g = 2.6 \times 10^{-9}$ W^{-1} cm $\times$ (laser intensity) from Ref. 17. These methods give consistent results, to within measurement uncertainties.

In the limiting case of $t_d \to \pm\infty$, the power spectrum of the optical phonon becomes

$$S_Q(\omega, t_d \to \pm\infty) = |\kappa_1|^2 I_{L1}I_S(2)^{3/2}\pi L(\Delta) \frac{1}{\Gamma^2 + (\omega - \Delta)^2} \quad (17)$$

(which is equivalent to the result given by Yuratich[18]), where the power spectrum of the effective (driving) field is the convolution of power spectra of $E_{L1}(t)$ and $E_S(t)$. To derive Eq. (17), we have made two assumptions. First, on the condition that $2\Gamma_{L1} \gg \Gamma_1/(gl)^{1/2}$, the Gaussian-shaped function in Eq. (11) can be treated as a delta function. Second, we have assumed that $2\Gamma_{L1} \gg \Gamma$, so that $L(\omega)$ can be replaced by $L(\Delta)$. According to Eq. (17), when $E_S(t)$ and $E_{L1}(t)$ are completely uncorrelated, the optical-phonon spectrum becomes the same as the Lorentzian Raman line shape. Although Eqs. (16) and (17) were derived by using the phase-diffusion model, they are actually valid for any purely phase-fluctuating pump field, if $L(\omega)$ is understood to be the self-convolution of the actual pump-field spectrum.

To see how the spectrum evolves between these two limits in the phase-diffusion model, we have numerically evaluated the combined Eqs. (8) and (15) and have plotted $S_Q(\omega)$ in Figs. 4(d), 4(e), and 4(f) for optical delays of 3.3, 37, and 160 psec, respectively. The laser linewidth was taken to be 9.0 GHz, as measured, and again the constants Γ, Γ_1, and g were evaluated by using Refs. 14 and 17. Good agreement is obtained between theory and experiment for small and large delays. For intermediate delay there is qualitative agreement, but there is a quantitative discrepancy in the ratio of the peak heights of the two components. This is most likely because the amplitude-stabilized chaotic light is not rigorously described by the phase-diffusion model. For example, the spectrum is known to be non-Lorentzian in the spectral tails.[13] The present experiment is sensitive to the detailed statistical nature of the pump field because it depends on a fourth-order correlation function in Eq. (12).

The existence of the narrow spectral component shows that laser phase fluctuations can be canceled out in anti-Stokes generation. Similar cancellations have been discussed for other nonlinear-optical processes, such as Raman Ramsey fringes,[19] two-photon absorption,[20] population trapping,[21] and optical double-resonance spectra.[22] Our observations also show that the phase fluctuations of the Stokes field do not follow those of the pump perfectly. If Stokes and pump fields were perfectly correlated, i.e., if $\xi(t)$ were a constant in Eq. (5), we would have observed a nearly monochromatic phonon with a spectral width that is independent of the Raman dephasing rate in the Stokes generator. The spectra that we have observed show that the width of the narrow spectral component depends on the Raman dephasing rate. The lack of perfect correlation is due to the collisional noise in the SRS process. That the generated Stokes field does not follow the pump field perfectly has also been shown in the case of a multimode laser, for which amplitude fluctuations dominate.[8]

CONCLUSION

In conclusion, in the coherent Raman scattering process the spectrum of the optical phonon, as observed in the anti-Stokes spectrum, depends on the degree of correlation between the two exciting fields: pump and Stokes. When the two fields are strongly correlated, as in the case when the Stokes field is produced in a Raman generator, the spectral shape of the optical phonon becomes the same as the gain-narrowed stimulated Raman line shape because the laser phase fluctuations cancel out totally, leaving only the collisional noise. This proves that the phase fluctuation of the Stokes field is not perfectly correlated to that of the pump. When the two fields are completely uncorrelated, as when the Stokes wave is delayed, the shape of the optical-phonon spectrum becomes the same as the Raman line shape because the effective driving field spectrum becomes broadband, and the molecules respond only within their linewidth. When the two fields are partially correlated, then the two spectral components appear together. The separation between the two components is the detuning from the Raman resonance, and the ratio of their peak heights is dependent on the degree of correlation between the two exciting fields. This study provides an experimental method to show directly not only the existence of phase correlation between pump field and generated Stokes field but also how strongly they are correlated.

The theory developed to interpret the experimental results is an extension of the quantum theory of SRS[6] to include anti-Stokes scattering and has been independently developed in Ref. 23. It is shown here that in the high-gain limit the quantum fluctuations of the generated fields can be thought of as arising from a classical noise process. In the case of low gain this not true, and certain nonclassical correlation effects have been predicted in this case.[24]

APPENDIX A: QUANTUM THEORY OF STOKES AND ANTI-STOKES GENERATION

Here we will provide a quantum-mechanical derivation that, in the high-gain limit, justifies treating the Stokes and anti-Stokes fields as classical quantities. To describe the Stokes and anti-Stokes generation process by the quantum theory, we will change $E_S(z,t)$, $E_{AS}(z,t)$, and $Q(z,t)$ to the operators $\hat{E}_S^{(-)}(z,t)$, $\hat{E}_{AS}^{(-)}(z,t)$, and $\hat{Q}(z,t)$, where the minus superscript means negative-frequency part. The laser field $E_{L1}(z,t)$ will still be treated classically. In the SRS generation process, the Stokes field operator at the output of Cell(1) can be expressed as[6]

$$\hat{E}_S^{(-)}(l,t) = \hat{E}_S^{(-)}(0,t) + \hat{\xi}(l,t)E_{L1}(t), \tag{A1}$$

where

$$\begin{aligned}\hat{\xi}(l,t) = {}& (\kappa_1\kappa_2 l)^{1/2}\int_0^t \mathrm{d}t' \exp[-\Gamma_1(t-t')]E_{L1}{}^*(t')\hat{E}_S^{(-)}(0,t') \\ &\times \frac{I_1(\{4\kappa_1\kappa_2 l[p(t)-p(t')]\}^{1/2})}{[p(t)-p(t')]^{1/2}} \\ &- i\kappa_2 \exp(-\Gamma_1 t)\int_0^l \mathrm{d}z' \hat{Q}^\dagger(z',0) I_0([4\kappa_1\kappa_2(l-z')p(t)]^{1/2}) \\ &- i\kappa_2 \int_0^t \mathrm{d}t' \int_0^l \mathrm{d}z' \exp[-\Gamma_1(t-t')]\hat{F}^\dagger(z',t') \\ &\times I_0(\{4\kappa_1\kappa_2(l-z')[p(t)-p(t')]\}^{1/2}),\end{aligned} \tag{A2}$$

where the $I_n(x)$ are modified Bessel functions and

$$p(t) = \int_0^t |E_{L1}(t'')|^2 \mathrm{d}t''. \tag{A3}$$

In the case of a smooth pulse, it is a good approximation that $p(t) = |E_{L1}|^2 t = I_{L1}t$. Γ_1 and $\hat{F}^\dagger$ describe the collision-induced damping and fluctuations. κ_1 and κ_2 are coupling constants in the SRS process defined in Refs. 6–9. The following properties of $\hat{Q}$ and $\hat{F}$ are assumed[6]:

$$\langle \hat{Q}^{\dagger}(z,0)\hat{Q}(z',0)\rangle = (AN)^{-1}\delta(z-z'), \quad \text{(A4)}$$

$$\langle \hat{F}^{\dagger}(z,t)\hat{F}(z',t')\rangle = 2\Gamma_1(AN)^{-1}\delta(z-z')\delta(t-t'), \quad \text{(A5)}$$

$$\langle \hat{Q}(z',0)\hat{Q}^{\dagger}(z,0)\rangle = \langle \hat{F}(z',t')\hat{F}^{\dagger}(z,t)\rangle = 0, \quad \text{(A6)}$$

$$\langle \hat{Q}^{\dagger}(z,0)\hat{F}(z',t')\rangle = \langle \hat{Q}^{\dagger}(z,0)\rangle\langle \hat{F}(z',t')\rangle = 0, \quad \text{(A7)}$$

$$\langle \hat{E}_S^{(+)}(0,t)\hat{F}^{\dagger}(z',t')\rangle = \langle \hat{F}(z,t)\hat{E}_S^{(-)}(0,t)\rangle = 0, \quad \text{(A8)}$$

where A is the cross-sectional area of the cylindrical interaction volume, N is the molecular number density, and $\langle\ \rangle$ means a quantum expectation value taken in the initial state. For the Stokes generator, the initial state is the vacuum state. In the high-gain limit, Eq. (A1) can be approximated as

$$\hat{E}_S^{(-)}(l,t) = \hat{\xi}(l,t)E_L(t), \quad \text{(A9)}$$

which is similar to Eq. (5) in the text.

The quantity of interest is the spectrum of the anti-Stokes field, which is the Fourier transform of the normally ordered autocorrelation function $\langle \hat{E}_{AS}^{(-)}(z,t+\tau)\hat{E}_{AS}^{(+)}(z,t)\rangle$. In the quantum theory the phase-matched contribution to the anti-Stokes field operator is given by

$$\hat{E}_{AS}^{(-)}(z,t) = \hat{E}_{AS}^{(-)}(0,t) - i\kappa_{2A}E_{L2}(t)z\int_0^t \exp[(i\Delta-\Gamma)(t-t')] \times E_{L1}(t')\hat{E}_S^{(+)}(l,t')\mathrm{d}t'. \quad \text{(A10)}$$

This results from solving the quantum version of Eqs. (1) and (2) of the text. Note that the negative-frequency part of the anti-Stokes field operator is proportional to the positive-frequency part of the Stokes field operator. This means that the normally ordered correlation function of the anti-Stokes field depends on the antinormally ordered correlation function of the Stokes field, i.e., $\langle \hat{E}_S^{(+)}(l,t')\hat{E}_S^{(-)}(l,t'')\rangle$. This quantity is nonzero, even for $l=0$. This is the origin of the statement that the anti-Stokes generation comes from the Stokes vacuum field fluctuations.[23]

On the other hand, the Stokes intensity and spectrum are proportional to the normally ordered quantity $\langle \hat{E}_S^{(-)}(l,t)\hat{E}_S^{(+)}(l,t+\tau)\rangle$, which in the high-gain limit is proportional to $\langle \hat{\xi}(t)\hat{\xi}^{\dagger}(t+\tau)\rangle$. The first term in Eq. (A2) gives only zero contribution to this autocorrelation function because the operator $\hat{E}_S^{(-)}(0,t)$ is the free-field operator, and its normally ordered autocorrelation $\langle \hat{E}_S^{(-)}(0,t)\hat{E}_S^{(+)}(0,t')\rangle$ in the vacuum state is zero. The second term in Eq. (A2) gives zero contribution to the autocorrelation in the steady state, also because of $\Gamma_1 t \gg 1$. Therefore the autocorrelation function of $\hat{\xi}(t)$ is equal to the autocorrelation of the third term in Eq. (A2). Note that the third term depends on the laser field only through $|E_L|^2$. So, for a temporally smooth pulse, $\langle \hat{\xi}(t)\hat{\xi}^{\dagger}(t+\tau)\rangle$ is independent of the pump-laser phase fluctuation. Thus this correlation function is the inverse Fourier transform of the Stokes power spectrum that occurs with a monochromatic laser field. This spectrum has been evaluated in Eq. (57) of Ref. 6, and its inverse transform is proportional to

$$\langle \hat{\xi}(t)\hat{\xi}^{\dagger}(t+\tau)\rangle = \frac{I_S}{I_{L1}}\exp\left(-\frac{\Gamma_1^2}{4gl}\tau^2\right), \quad \text{(A11)}$$

where I_S is the Stokes intensity

$$I_S = \frac{2\pi\hbar\omega_S}{Ac}\frac{\Gamma_1}{2(\pi gl)^{1/2}}e^{gl}, \quad \text{(A12)}$$

$g = 2\kappa_1\kappa_2 I_{L1}/\Gamma_1$, and $I_{L1} = |E_{L1}|^2$.

Now, returning to the anti-Stokes field, we recall that we must evaluate the antinormally ordered correlation function $\langle \hat{\xi}^{\dagger}(t+\tau)\hat{\xi}(t)\rangle$. Only the first term in Eq. (A2) gives a nonzero contribution to this function because of Eqs. (A6) and (A8). We find that

$$\begin{aligned}\langle \hat{\xi}^{\dagger}(t+\tau)\hat{\xi}(t)\rangle = \kappa_1\kappa_2 z\int_0^{t+\tau}\mathrm{d}t'\int_0^t \mathrm{d}t''\exp[-\Gamma_1(2t+\tau-t'-t'')] \\ \times \langle E_L(t')E_L{}^*(t'')\rangle\langle \hat{E}_S^{(+)}(0,t')\hat{E}_S^{(-)}(0,t'')\rangle \\ \times \frac{I_1(\{4\kappa_1\kappa_2 l[p(t+\tau)-p(t')]\}^{1/2})}{[p(t+\tau)-p(t')]^{1/2}} \\ \times \frac{I_1(\{4\kappa_1\kappa_2 l[p(t)-p(t'')]\}^{1/2})}{[p(t)-p(t'')]^{1/2}}. \quad \text{(A13)}\end{aligned}$$

For the one-dimensional, free-field operator of the Stokes field, the commutator is[25,26]

$$[\hat{E}_S^{(+)}(0,t'), \hat{E}_S^{(-)}(0,t'')] = \frac{2\pi\hbar\omega_S}{Ac}\delta(t'-t''). \quad \text{(A14)}$$

When Eq. (A14) is used, Eq. (A13) becomes

$$\langle \hat{\xi}^{\dagger}(t+\tau)\hat{\xi}(t)\rangle = \frac{2\pi\hbar\omega_S}{Ac}\frac{f(\tau)}{I_{L1}}, \quad \text{(A15)}$$

where

$$f(\tau) = \frac{(\alpha z)^2}{4}\exp(-\Gamma_1\tau)\int_0^{\infty}\mathrm{d}t'\exp(-2\Gamma_1 t')\frac{I_1([\alpha l t']^{1/2})}{[\alpha l t']^{1/2}} \times \frac{I_1([\alpha l(t'+\tau)]^{1/2})}{[\alpha l(t'+\tau)]^{1/2}}, \quad \text{(A16)}$$

where $\alpha = 2g\Gamma_1$. We have replaced $t-t'$ with t' and have assumed that t is ∞ for the steady state. The Fourier transform of $f(\tau)$ is

$$P(\omega) = \frac{1}{\pi}\mathrm{Re}\int_0^{\infty} f(\tau)e^{-i\omega\tau}\mathrm{d}\tau. \quad \text{(A17)}$$

If we use the asymptotic form of the modified Bessel function $I_n(x) = e^x/(2\pi x)^{1/2}$ for $x \gg 1$, and refer to the method leading to Eq. (54) of Ref. 6, the power spectrum then becomes

$$P(\omega) = \frac{1}{4\pi^2}\mathrm{Re}\frac{(\alpha l)^2}{4}\left|\int_0^{\infty}\mathrm{d}t' e^{i\omega t'}e^{-\Gamma t'}\frac{\exp[(\alpha l t')^{1/2}]}{(\alpha l t')^{3/4}}\right|^2. \quad \text{(A18)}$$

The integral is meant to be carried out only over the region near $t' = \alpha l/4\Gamma_1^2$, where the integrand is strongly peaked. Then, by using the method leading to Eq. (56) of Ref. 6, this becomes

$$P(\omega) \simeq \frac{1}{2\pi}e^{gl}\exp\left(-\frac{gl}{\Gamma_1^2}\omega^2\right), \quad \text{(A19)}$$

whose inverse transform leads to

$$\langle \hat{\xi}^{\dagger}(t+\tau)\hat{\xi}(t)\rangle = \frac{I_S}{I_{L1}} \exp\left(-\frac{{\Gamma_1}^2}{4gl}\tau^2\right). \tag{A20}$$

Thus we see that in the high-gain limit the antinormally ordered correlation function [Eq. (A20)] equals the normally ordered correlation function [Eq. (A11)]. This is a form of the correspondence principle, which says that when many photons are present in an amplifier the quantum-mechanical nature of the field is unimportant.[27] This justifies treating the $\hat{\xi}(t)$ operator as a classical random process $\xi(t)$, with correlation function $\langle \xi(t+\tau)\xi^*(t)\rangle$ given by Eq. (A11) or Eq. (A20). Note that this correlation function is independent of any phase fluctuation in the laser field $E_{L1}(t)$. The power spectrum of $\xi(t)$ is then given by Eq. (11) of the text.

ACKNOWLEDGMENT

This research was supported by the U.S. Army Research Office.

* Permanent address, Department of Physics, Warsaw University, Warsaw, Poland.

† Present address, Department of Physics, University of Oregon, Eugene, Oregon 97403.

REFERENCES

1. R. L. Carman, F. Shimizu, C. S. Wang, and N. Bloembergen, Phys. Rev. A **2**, 60 (1970).
2. M. G. Raymer, J. Mostowski, and J. L. Carlsten, Phys. Rev. A **19**, 2304 (1979).
3. S. A. Akhamanov, Yu. E. D'yakov, and L. I. Pavlov, Sov. Phys. JETP **39**, 249 (1974); J. Eggleston and R. L. Byer, IEEE J. Quantum Electron. **QE-16**, 850 (1980); G. P. Dzhotyan, Yu. E. D'yakov, I. G. Zubarev, A. B. Mironov, and S. I. Mikhailov, Sov. Phys. JETP **46**, 431 (1977); Sov. J. Quantum Electron. **7**, 783 (1977).
4. E. A. Stappaerts, W. H. Long, Jr., and H. Komine, Opt. Lett. **5**, 4 (1980); J. Rifkin, M. L. Bernt, D. C. MacPherson, and J. L. Carlsten, J. Opt. Soc. Am. B **5**, 1607 (1988).
5. G. G. Lombardi and H. Injeyan, J. Opt. Soc. Am. B **3**, 1461 (1986); M. D. Duncan, R. Mahon, L. L. Tankersley, and J. Reintjes, J. Opt. Soc. Am. B **5**, 37 (1988).
6. J. Mostowski and M. G. Raymer, Opt. Commun. **36**, 237 (1981); M. G. Raymer and J. Mostowski, Phys. Rev. A **24**, 1980 (1981).
7. M. G. Raymer and L. A. Westling, J. Opt. Soc. Am. B **2**, 1417 (1985).
8. L. A. Westling and M. G. Raymer, Phys. Rev. A **32**, 4835 (1987).
9. M. Trippenbach, K. Rzazewski, and M. G. Raymer, J. Opt. Soc. Am. B **1**, 671 (1984).
10. Z. W. Li, C. Radzewicz, and M. G. Raymer, Opt. Lett. **13**, 491 (1988).
11. L. A. Rahn, R. L. Farrow, and R. P. Lucht, Opt. Lett. **9**, 233 (1984); G. S. Agarwal and S. Singh, Phys. Rev. A **25**, 3195 (1982); G. S. Agarwal and R. L. Farrow, J. Opt. Soc. Am. B **4**, 1596 (1986); R. J. Hall, Opt. Commun. **56**, 127 (1985).
12. A. Laubereau and W. Kaiser, Rev. Mod. Phys. **50**, 607 (1978).
13. C. Radzewicz, Z. W. Li, and M. G. Raymer, Phys. Rev. A **37**, 2039 (1988).
14. W. K. Bischel and M. J. Dyer, Phys. Rev. A **33**, 3113 (1986).
15. M. Takatsuji, Phys. Rev. A **11**, 619 (1975).
16. M. G. Raymer and J. Cooper, Phys. Rev. A **20**, 2238 (1979).
17. W. K. Bischel and M. J. Dyer, J. Opt. Soc. Am. B **3**, 677 (1986).
18. M. A. Yuratich, Molec. Phys. **38**, 625 (1979).
19. J. E. Thomas, P. R. Hemmer, S. Ezekiel, C. C. Leiby, Jr., R. H. Picard, and C. R. Willis, Phys. Rev. Lett. **48**, 867 (1982).
20. A. M. Bonch-Bruevich, S. G. Przhibel'skii, and N. A. Chigir', Sov. Phys. JETP **65**, 439 (1987).
21. B. J. Dalton and P. L. Knight, Opt. Commun. **42**, 411 (1982).
22. T. A. Kennedy and S. Swain, J. Phys. B **17**, L389 (1984).
23. S. Ya. Kilin, Europhys. Lett. **5**, 419 (1988).
24. J. Perina, Opt. Acta **28**, 1529 (1981).
25. Z. Y. Ou, C. K. Hong, and L. Mandel, J. Opt. Soc. Am. B **4**, 1574 (1987).
26. D. Polder, M. F. H. Schuurmans, and Q. H. F. Vrehen, Phys. Rev. A **19**, 1192 (1979).
27. C. K. Hong, S. Friberg, and L. Mandel, J. Opt. Soc. Am. B **2**, 494 (1985).